

Roles of spin fluctuation and frustration in the superconductivity of β -(BDA-TTP) $_2X$ ($X=\text{SbF}_6, \text{AsF}_6$) under uniaxial compression

Hiroshi Ito, Tetsuo Ishihara, Hisaaki Tanaka, Shin-ichi Kuroda, Takeo Suzuki, Seiichiro Onari, and Yukio Tanaka
Department of Applied Physics, Nagoya University, Chikusa, Nagoya 464-8603, Japan

Jun-ichi Yamada

Department of Material Science, University of Hyogo, 3-2-1 Kouto, Kamigori-cho, Hyogo 678-1297, Japan

Koichi Kikuchi

Department of Chemistry, Tokyo Metropolitan University, 1-1 Minami-Ohsawa, Hachioji 192-0397, Japan

(Received 31 July 2008; revised manuscript received 23 October 2008; published 14 November 2008)

β -type BDA-TTP [BDA-TTP=2,5-bis(1,3-dithian-2-ylidene)-1,3,4,6-tetrathiapentalene] salts possess high transition temperatures T_C reaching 7 K among organic superconductors. T_C of β -(BDA-TTP) $_2X$ ($X=\text{SbF}_6, \text{AsF}_6$) is studied by resistive measurements under uniaxial compression. T_C once increases and takes a maximum under compression parallel to the donor stack while it decreases under compression perpendicular to the donor stack. These results are in agreement with the half-filled Hubbard model on the triangular lattice in which the compression controls the spin fluctuation and frustration in the weak pressure region.

DOI: 10.1103/PhysRevB.78.172506

PACS number(s): 74.70.Kn, 74.62.Fj, 74.20.Mn

The superconductivity of the high- T_C κ -type BEDT-TTF salts is believed to arise from the spin fluctuation in terms of the half-filled Hubbard model on an anisotropic triangular lattice.¹⁻³ In κ -type donor arrangements, donors form dimers. The split antibonding highest occupied molecular orbital (HOMO) band is half-filled with the effective on-site Coulomb energy (U) close to the bandwidth (W). It is a strongly correlated system with enhanced antiferromagnetic spin fluctuations in terms of the Mott physics.⁴ The dimers are arranged on the anisotropic triangular lattice in which the spin frustration plays an important role.^{1,3,5} The superconductivity is suppressed when the frustration on the triangular lattice becomes strong.

Meanwhile, β -type BDA-TTP [BDA-TTP=2,5-bis(1,3-dithian-2-ylidene)-1,3,4,6-tetrathiapentalene] [see Fig. 1(a)] salts have attracted attention owing to the relatively high T_C among organic superconductors.⁶ β -type BDA-TTP salts share structural similarities with the BEDT-TTF salts.⁶ The BDA-TTP molecules are packed in layers in a β -type arrangement, having donor stacks along the $a+c$ axis, as shown in Fig. 1(b). Unconventional d -wave superconductivity similar to the BEDT-TTF salts has been suggested by the specific heat⁷ and scanning tunneling microscope (STM) measurements.⁸

The BDA-TTP salts are the key materials for understanding how the dimerized BEDT-TTF is a prerequisite for high T_C in organic superconductors, since they have two distinct properties different from κ -type BEDT-TTF salts. One is the structure of the donor molecule. The BDA-TTP salt is an organic superconductor in which the donor molecule is not based on the tetrachalcogenafulvalene structure. The other is the β -type donor arrangement. In the β -type structure, the donors dimerize, forming a triangular lattice as shown in Fig. 1(c). However, the dimerization of the molecules is not so strong as the κ -type salts. For the present salts, the intradimer transfer integral is calculated by the extended Hückel method as $t_{p1}=-0.147, -0.151$ eV for $X=\text{SbF}_6$ and

$X=\text{AsF}_6$, respectively, compared with other interdimer integrals $t_{p2}=-0.0623, -0.0754$ eV, $t_{q1}=-0.0818, -0.0837$ eV, $t_{q2}=-0.0889, -0.0962$ eV, and $t_c=0.00447, 0.00337$ eV.⁹ Since the splitting between the bonding and antibonding HOMO bands is small (0.06 eV) compared with the bandwidth, β -type salts are a borderline material with regard to whether they can be treated with a half-filled model. Incidentally, superconductivity at 14.2 K, which is higher than for κ -type salts, has been reported for β' -(BEDT-TTF) $_2\text{ICl}_2$ under a hydrostatic pressure of 8.2 GPa.¹⁰ The superconductivity of β -type salts attracts attention in the sense that the dimerization-induced half-filled electronic structure with enhanced spin fluctuation is a prerequisite for high T_C . As a

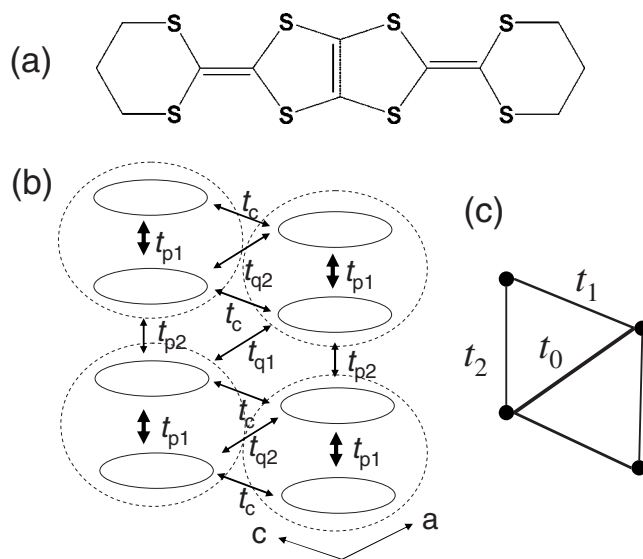


FIG. 1. (a) The BDA-TTP molecule. (b) The arrangement of molecules and the transfer integrals between the molecules within the conduction layer of β -(BDA-TTP) $_2X$. The ellipses represent BDA-TTP molecules. The dotted ellipses indicate dimers. (c) The triangular-lattice structure taking the dimer as a unit.

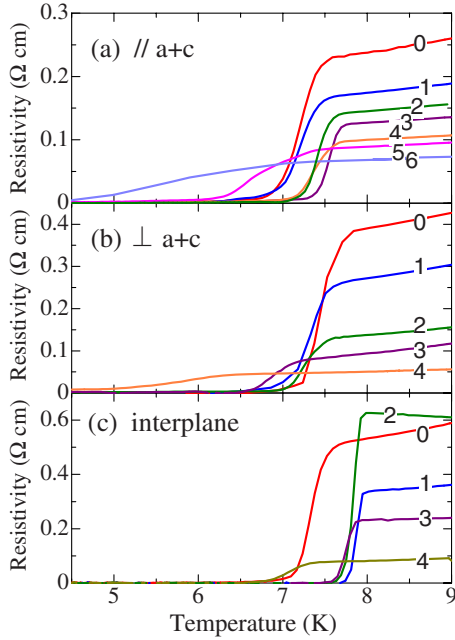


FIG. 2. (Color online) The resistive transition for $X=\text{SbF}_6$ under in-plane compression (a) parallel and (b) perpendicular to $a+c$ and (c) under interplane compression. The number on each curve denotes the piston pressure in kbar. The curve “0” indicates the transition under epoxy encapsulation before applying piston pressure.

model for the superconductivity of $\beta\text{-(BDA-TTP)}_2X$, the effectively half-filled extended Hubbard model similar to that for the κ -type BEDT-TTF salts is proposed in which spin and charge fluctuations induce d_{xy} -wave superconductivity.⁹

Uniaxial compression is a unique method for gaining insight into the phase diagram of low-dimensional conductors since we can access each transfer integral selectively.¹¹ The T_C variations under uniaxial compression for κ -type BEDT-TTF salts^{12–14} are explained in terms of the anisotropic triangular-lattice model.¹⁵ The results for three different salts align so that T_C peaks at the anisotropy of 0.7. This result is in agreement with the fluctuation-exchange (FLEX) calculation based on the half-filled Hubbard model in which T_C takes a maximum as a result of the interplay between the enhancement of spin fluctuation and spin frustration.¹ In this Brief Report we report the uniaxial compression effect on the T_C of $\beta\text{-(BDA-TTP)}_2X$ ($X=\text{SbF}_6, \text{AsF}_6$) and discuss the results in terms of the half-filled Hubbard model in view of the role of spin fluctuation and spin frustration.

Samples were prepared electrochemically.⁶ Single crystals were aligned with respect to the compression direction with the help of a stripelike pattern on the ac plane. The direction of the stripe was found to be perpendicular to $a+c$ by x-ray and electron spin resonance (ESR) measurements. Interlayer four-probe resistivity measurements under uniaxial compression were performed by the epoxy-encapsulation method¹¹ described previously.¹² Two to three samples from different batches were measured for each compression direction to ensure reproducibility. For the hydrostatic pressure measurement, the sample was set in a Teflon cap filled with a Daphne 7373 oil.

In Fig. 2, we show the interplane resistivity near T_C under

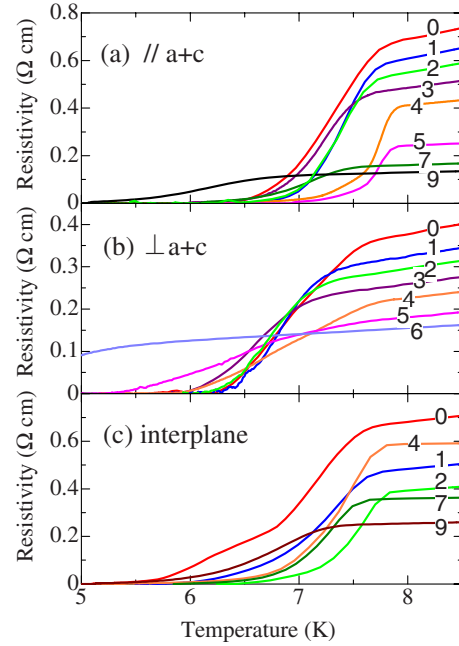


FIG. 3. (Color online) The resistive transition for $X=\text{AsF}_6$ under in-plane compression (a) parallel and (b) perpendicular to $a+c$ and (c) under interplane compression. The number on each curve denotes the piston pressure in kbar. The curve “0” indicates the transition under epoxy encapsulation before applying piston pressure.

uniaxial compression parallel and perpendicular to $a+c$ and under interplane compression for $X=\text{SbF}_6$. In Figs. 4(a) and 4(c), we show the piston pressure dependence of T_C of $X=\text{SbF}_6$ defined as the midpoints of the resistive transition. Upper and lower error bars represent the onset and offset points of the transition. Under in-plane compression parallel to $a+c$ (parallel compression), T_C increases gradually by 0.5 K up to 3 kbar and decreases under further piston pressure. Under in-plane compression perpendicular to $a+c$ (perpendicular compression), T_C decreases gradually up to 2.5 kbar and then decreases rapidly under further piston pressure. Under interplane compression, T_C rapidly increases up to a piston pressure of 0.5 kbar, remains high up to ~ 3 kbar, and decreases under further piston pressure. Under high piston pressures, the transition width increases for every compression direction. The overall behaviors of T_C under uniaxial compression agree qualitatively with magnetization measurements.¹⁶ Because T_C increases under interplane compression but remains almost unchanged under in-plane compression up to 1 kbar, it is expected that T_C will increase under hydrostatic pressure. In fact, a 0.4 K increase in T_C is observed under a hydrostatic pressure of 0.5 kbar.

In Fig. 3, we show the interplane resistivity near T_C under uniaxial compression parallel and perpendicular to $a+c$ and under interplane compression for $X=\text{AsF}_6$. In Figs. 4(b) and 4(d), we show the piston pressure dependence of T_C for $X=\text{AsF}_6$ defined as the midpoints of the resistive transition. Upper and lower error bars represent the onset or offset points of the transition. Although the resistive transitions are broader than those for $X=\text{SbF}_6$, it is found that T_C increases up to 4 kbar and decreases above 5 kbar under parallel compression, except for a minimum at ~ 3 kbar. Under perpen-

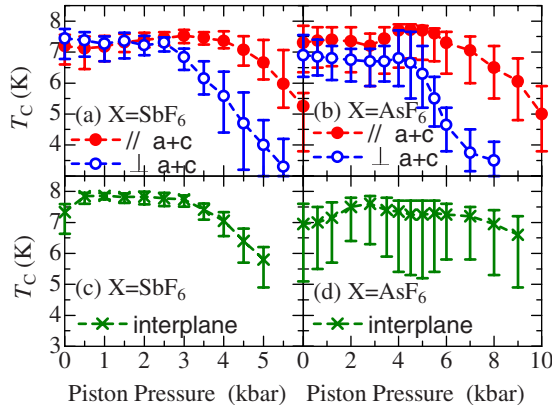


FIG. 4. (Color online) The changes in T_C defined by the mid-points of the transition under compression parallel and perpendicular to $a+c$ for (a) $X=\text{SbF}_6$ and (b) $X=\text{AsF}_6$ and under interplane compression for (c) $X=\text{SbF}_6$ and (d) $X=\text{AsF}_6$. Upper and lower error bars represent the onset and offset points of the transition. The origin of the horizontal axis corresponds to T_C under epoxy encapsulation before applying piston pressure. The broken lines are guides for the eyes.

dicular compression, T_C decreases gradually up to 4 kbar and rapidly above 5 kbar, except for a minimum at ~ 3 kbar. Under interplane compression, T_C increases up to 2 kbar, remains high up to ~ 6 kbar, and decreases under further piston pressure.

It is noted that T_C increases from 6.8 to 7.5 K for $X=\text{SbF}_6$ and from 6.2 to 6.9 K for $X=\text{AsF}_6$ when the sample is embedded in epoxy resin before applying piston pressure. This may be because an additional compression is applied to the crystal by the epoxy. When the epoxy solidifies, a volume contraction may occur. Furthermore, additional thermal contraction is applied to the crystal by cooling. The thermal contraction of the crystal from room temperature to 12 K is found to be 0.8%–1% by x-ray measurements. The contraction difference with stycast 1266 (1.2% thermal contraction¹⁷) is 0.2%–0.4%, which corresponds to an additional pressure of 1 kbar applied to the crystal by cooling considering the compressibility of the crystal.¹⁸ Since interplane compression is most effective in increasing T_C in this weak pressure range, the T_C increase in epoxy is mainly caused by compression along the interplane direction.

In order to understand the results in terms of theoretical models, the transfer integrals under uniaxial compression are calculated by the extended Hückel method assuming a uniform displacement of molecules. The compressibility is assumed to be 0.3%/kbar referring to the results for $\beta\text{-(BEDT-TTF)}_2\text{I}_3$.¹⁸ For the calculation, we assume that the shape of the molecule is not changed and only the separation between molecules is reduced under compression. We assume that 1 kbar of hydrostatic pressure is already applied by the epoxy before the application of the external compression. Here we apply the half-filled Hubbard model with dimerized donors on the triangular lattice. The calculated transfer integrals are mapped onto the triangular lattice with the parameters $t_0 = -t_{q1}/2$, $t_1 = -t_{q2}/2 + t_c$, and $t_2 = -t_{p2}/2$ shown in Fig. 1(c) with an effective on-site Coulomb interaction of $U_{\text{eff}} = 2t_{p1}$.¹⁹ In Fig. 5, we show the variation of these parameters under uniaxial compression.

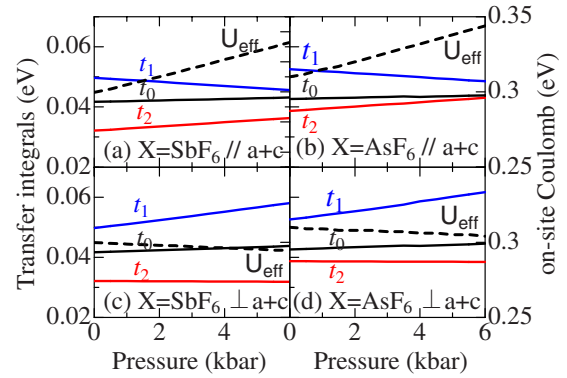


FIG. 5. (Color online) Calculated transfer integrals t_0 , t_1 , and t_2 consisting of a triangular lattice (solid lines) and the effective on-site Coulomb interaction (broken lines) under uniaxial compression parallel and perpendicular to $a+c$ for (a), (c) $X=\text{SbF}_6$ and (b), (d) $X=\text{AsF}_6$.

In Fig. 6, we show the normalized variation in T_C calculated by the FLEX approximation for $X=\text{SbF}_6$ and $X=\text{AsF}_6$, together with those observed as midpoints of the resistive transition. The superconductivity is induced by the spin fluctuation with the d -wave gap function. Under parallel compression, the calculated T_C once increases and takes a maximum at 3 kbar for $X=\text{SbF}_6$ and 1.5 kbar for $X=\text{AsF}_6$ and then decreases under further pressure. The maximum of T_C is a result of the competition between the enhancement of the spin fluctuation and the spin frustration, similar to κ -type BEDT-TTF salts.^{1,15} Under parallel compression, t_{p1} and t_{p2} increase. The spin fluctuation is enhanced by the increase in U_{eff} . The spin frustration is also enhanced since the three transfer integrals, t_0 , t_1 , and t_2 , tend to merge toward high pressure as shown in Figs. 5(a) and 5(b). The presence of the

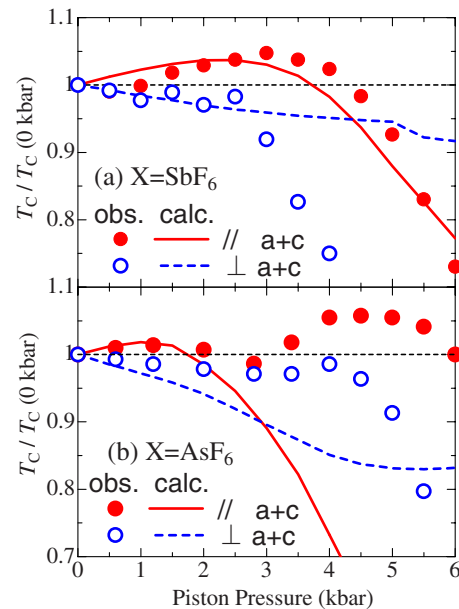


FIG. 6. (Color online) The normalized variation in T_C calculated (solid and broken lines) and observed (midpoint, closed and open circles) under uniaxial compression parallel and perpendicular to $a+c$ for (a) $X=\text{SbF}_6$ and (b) $X=\text{AsF}_6$.

T_C maximum agrees with the observed T_C . On the other hand, the calculated T_C decreases monotonously under perpendicular compression. The decrease of T_C is caused by the decrease in spin fluctuation in spite of the release of the spin frustration. Under perpendicular compression, t_{q1} and t_{q2} increase. The spin fluctuation is suppressed due to a relative decrease in U/W , while the spin frustration weakens since the three integrals deviate from each other as shown in Figs. 5(c) and 5(d). Except for the T_C minimum found for $X = \text{AsF}_6$, the decrease of T_C agrees with the observed T_C .

In the present calculation, the calculated T_C deviates from the observed T_C above 3 kbar; the observed T_C under perpendicular compression decreases more rapidly than that calculated for $X = \text{SbF}_6$; the T_C minima at 3 kbar and subsequent increase are not reproduced by the calculation for $X = \text{AsF}_6$; the calculated T_C for $X = \text{AsF}_6$ decreases much faster than that for $X = \text{SbF}_6$, which is opposite to the experimental trend. These discrepancies may stem from the assumption of the uniform displacement of molecules which may not be valid at high pressures. For the difference in the pressure range of the T_C decrease at the high-pressure region, a possible difference in the compressibility for the two salts may be considered. As for the origin of the T_C minima in $X = \text{AsF}_6$, possible structural transition cannot be ruled out. For further study to understand the T_C behavior in terms of the displacement of molecules, structural studies under uniaxial compression are desirable. As a reason for the larger discrepancy between the calculated and the observed found for perpendicular compression, it is noted that the single band picture may become inappropriate because of the decrease in U/W . More elaborate theoretical studies are underway including the use of two-band models.²⁰

The interplane compression effects on the superconductivity demonstrate the importance of the three dimensionality of the superconductivity, which has not been taken into consideration by theory. The increase in T_C due to weak interplane pressure corresponds to the positive jump in the interplane thermal-expansion coefficient in terms of the Ehrenfest relation, in contrast to BEDT-TTF salts.²¹ The presence of a broad magnetoresistance peak under a magnetic field almost parallel to the ac plane indicates that the interplane transfer integral is 1 order of magnitude larger than that of BEDT-TTF salts.²² The interplane effects may be caused by the trimethylene bases at both ends of the BDA-TTP molecule, which enhance the interlayer interaction in comparison with the BEDT-TTF salts.

In summary, the uniaxial compression dependence of T_C has been measured resistively for the organic superconductor β -(BDA-TTP)₂X ($X = \text{SbF}_6, \text{AsF}_6$). In both salts, T_C once increases and takes a maximum under compression parallel to the donor stack and T_C decreases under compression perpendicular to the donor stack. These results are in agreement with the half-filled Hubbard model on the triangular lattice in which the enhancements of the spin fluctuation and the spin frustration play important roles in the weak pressure region. Under interplane compression, T_C increases by 0.5 K up to 2 kbar for both salts, demonstrating the importance of the interlayer interaction.

The authors wish to thank M. Umemiya for performing the x-ray analysis. The authors also thank Y. Suzumura for theoretical discussions. This research was supported by the Scientific Research on Priority Areas "Novel Functions of Molecular Conductors under Extreme Conditions" under Contract No. 18028012 of MEXT, Japan.

¹H. Kino and H. Kontani, J. Phys. Soc. Jpn. **67**, 3691 (1998).

²H. Kondo and T. Moriya, J. Phys. Soc. Jpn. **67**, 3695 (1998); **68**, 3170 (1999).

³B. J. Powell and R. H. McKenzie, J. Phys.: Condens. Matter **18**, R827 (2006), and references therein.

⁴K. Kanoda, Hyperfine Interact. **104**, 235 (1997).

⁵T. Watanabe, H. Yokoyama, Y. Tanaka, and J. Inoue, J. Phys. Soc. Jpn. **75**, 074707 (2006).

⁶J. Yamada, M. Watanabe, H. Akutsu, S. Nakatsuji, H. Nishikawa, I. Ikemoto, and K. Kikuchi, J. Am. Chem. Soc. **123**, 4174 (2001).

⁷Y. Shimojo, T. Ishiguro, T. Toita, and J. Yamada, J. Phys. Soc. Jpn. **71**, 717 (2002).

⁸R. Muraoka, K. Nomura, K. Ichimura, T. Toita, and J. Yamada (unpublished).

⁹Y. Nonoyama, Y. Maekawa, A. Kobayashi, Y. Suzumura, and H. Ito, J. Phys. Soc. Jpn. **77**, 094703 (2008).

¹⁰H. Taniguchi, M. Miyashita, K. Uchiyama, K. Satoh, N. Mori, H. Okamoto, K. Miyagawa, K. Kanoda, M. Hedo, and Y. Uwatoko, J. Phys. Soc. Jpn. **72**, 468 (2003).

¹¹M. Maesato, Y. Kaga, R. Kondo, and S. Kagoshima, Rev. Sci. Instrum. **71**, 176 (2000).

¹²H. Ito, Y. Hasegawa, A. Ishihara, S. Takasaki, J. Yamada, and H.

Anzai, Synth. Met. **133**, 233 (2003).

¹³T. Ishikawa, M. Maesato, and G. Saito, Synth. Met. **133**, 227 (2003).

¹⁴T. Mizutani, M. Tokumoto, T. Kinoshita, J. S. Brooks, Y. Uwatoko, O. Drozdova, K. Yakushi, I. Tamura, H. Kobayashi, T. Mangetsu, J. Yamada, and K. Ishida, Synth. Met. **133**, 229 (2003).

¹⁵M. Maesato, Y. Shimizu, T. Ishikawa, and G. Saito, Synth. Met. **137**, 1243 (2003).

¹⁶M. Tokumoto, T. Mizutani, Y. V. Sushko, Y. Uwatoko, K. Yamamoto, K. Yakushi, J. Yamada, and K. Ishida, Presented at ICSM'06, Dublin, 2006 (unpublished).

¹⁷G. W. Swift and R. E. Packard, Cryogenics **19**, 362 (1979).

¹⁸H. Tanino, K. Kato, M. Tokumoto, H. Anzai, and G. Saito, J. Phys. Soc. Jpn. **54**, 2390 (1985).

¹⁹H. Kontani, Phys. Rev. B **67**, 180503(R) (2003).

²⁰T. Suzuki, S. Onari, H. Ito, and Y. Tanaka (unpublished).

²¹J. Müller, M. Lang, J. A. Schlueter, U. Geiser, and D. Schweitzer, Synth. Met. **120**, 855 (2001).

²²E. S. Choi, E. Jobilong, A. Wade, E. Goetz, J. S. Brooks, J. Yamada, T. Mizutani, T. Kinoshita, and M. Tokumoto, Phys. Rev. B **67**, 174511 (2003).